An experimental study of the gas-phase reaction between Cl atoms and trans-2-pentenal: Kinetics, products and SOA formation

Asma Grira, M. Antiñolo, André Canosa, Alexandre Tomas, E. Jiménez, Gisèle El Dib

An experimental study of the gas-phase reaction between Cl atoms and *trans-2*-pentenal: kinetics, products and SOA formation

Asma Grira[1,2], María Antiñolo[3,4,*#], André Canosa[1], Alexandre Tomas[2], Elena Jiménez[3,4], Gisèle El Dib[1,*]

[1]*CNRS, IPR (Institut de Physique de Rennes)-UMR 6251. Université de Rennes, F-35000 Rennes, France*

[2]*IMT Lille Douai, Institut Mines-Télécom, Univ. Lille, Center for Energy and Environment, F-59000 Lille, France*

[3]*Departamento de Química Física, Facultad de Ciencias y Tecnologías Químicas, Universidad de Castilla-La Mancha, Avda. Camilo José Cela 1B, E-13071, Ciudad Real, Spain*

[4]*Instituto de Investigación en Combustión y Contaminación Atmosférica (ICCA), Universidad de Castilla-La Mancha, Camino de Moledores s/n, E-13071, Ciudad Real, Spain*

[#]Currently at: Escuela de Ingeniería Industrial y Aeroespacial, Universidad de Castilla-La Mancha, Avenida Carlos III s/n. Real Fábrica de Armas. E-45071, Toledo, Spain.

*Corresponding authors:

Gisèle El Dib Phone: +33 2 23 23 56 80; email: gisele.eldib@univ-rennes1.fr

Maria Antinolo Phone: +34 9 26 29 53 00; Ext. 3446; email: Maria.Antinolo@uclm.es

Abstract

The gas-phase reaction of trans-2-pentenal (T2P) with Cl atoms was studied at atmospheric pressure and room temperature. A rate coefficient of $(2.56\pm0.83)\times10^{-10}$ cm^3 $molecule^{-1}$ s^{-1} was obtained using the relative rate method and isoprene, cyclohexane and ethanol as reference compounds. The kinetic study was carried out using a 300-L Teflon bag simulation chamber (IMT Lille Douai-France) and a 16-L Pyrex cell (UCLM-Ciudad Real-Spain), both coupled to the Fourier transform infrared (FTIR) technique. Gas-phase products and secondary organic aerosol (SOA) formation were studied at UCLM using a 16-L Pyrex cell and a 264-L quartz simulation chamber coupled to the FTIR and gas-chromatography-mass spectrometry (GC-MS) techniques. HCl, CO, and propanal were identified as products formed from the studied reaction and quantified by FTIR, being the molar yield of the latter (5.2±0.2)%. Formic acid was identified as a secondary product and was quantified by FTIR with a yield of (6.2±0.4)%. In addition, 2-chlorobutanal and 2–pentenoic acid were identified, but not quantified, by GC-MS as products. The SOA formation was investigated using a fast mobility particle sizer spectrometer. The observed SOA yields reached maximum values of around 7% at high particle mass concentrations. This work provides the first study of the formation of gaseous and particulate products for the reaction of Cl with T2P. A reaction mechanism is suggested to explain the formation of the observed gaseous products. The results are discussed in terms of the structure-reactivity relationship, and the atmospheric implications derived from this study are commented as well.

Keywords: Unsaturated aldehyde, kinetics, mechanism, organic aerosols, atmospheric lifetimes

1. Introduction

It is well known that non-methane biogenic volatile organic compounds (BVOCs) account for approximately 90% of VOCs present in the atmosphere. BVOCs play an important role in the chemistry of the troposphere since their oxidation provides major reaction pathways for the formation of Secondary Organic Aerosols (SOAs) (Hoffmann et al., 1997, Griffin et al., 1999). In addition, the reactivity of BVOCs has an impact on the HO_x (OH + HO_2), NO_x (NO + NO_2) and the tropospheric ozone budgets. Therefore, it is important to understand the oxidation of BVOCs in the atmosphere to assess their role in the troposphere's chemistry. This is crucial for atmospheric models to predict the formation of atmospheric photo-oxidants, SOA and the HO_x cycle (Kanakidou et al., 2005, Rudich et al., 2007).

Unsaturated aldehydes are BVOCs that may be emitted into the atmosphere from the enzymatic oxidation of linolenic and linoleic acids present in vegetation in response to stress (Winer et al. 1992, Hatanaka, 1993, Heiden et al., 2003, Seco et al., 2007).

They may also be formed in situ as a result of the oxidation of dienes in the atmosphere (Orlando and Tyndall, 2002). Besides their emission from biogenic sources, unsaturated aldehydes are also emitted into the atmosphere from anthropogenic sources such as the combustion of wood, polymers, tobacco and gasoline (Magneron et al., 2002) and from chemical industries (Graedel and Crutzen, 1986).

Atmospheric mixing ratios of unsaturated aldehydes are in the order of ppb. For instance, the mixing ratio of acrolein, the smallest unsaturated aldehyde, in several cities was reported to be up to 12 ppb (Seaman et al., 2006, Faroon et al., 2008). Larger unsaturated aldehydes, such as trans-2-pentenal (T2P), have also been detected in the atmosphere with mixing ratios of a few ppb in soybean seeds after anaerobic incubation (Gardner et al., 1996). T2P is also emitted by vegetation such as orange (Moshonas et al., 1973), tomato (Tandon et al., 2000) and black tea (Yamanishi et al., 1972). Besides, T2P is emitted directly from food products such as olive oil

(Angerosa et al., 2000, Masella et al., 2019), milk powder (Cheng et al., 2019), wine (Saison et al., 2009, Martins et al., 2013), dry sausages, cheese and bread (Bianchi et al., 2007) or during food preparation as clam frying (Cheng et al., 2019). T2P has also been detected in human breath (Ruzsanyi et al., 2002) and cigarette smoke (Hatai et al., 2019). Further, this species is used to protect crop plants from pests and weeds (Rodríguez-Kabana et al., 2008).

Like other unsaturated aldehydes, once emitted into the atmosphere, T2P is expected to be removed mainly by reaction with OH and NO_3 radicals and by photolysis during the daytime (Houk, 1976, Calvert et al., 2011). However, reactions with chlorine (Cl) atoms may play an important role in the removal of these species in the atmosphere and maybe competitive with those due to the OH radicals. Heterogeneous $ClNO_2$ formation in polluted environments has been shown as a major route for the production of reactive gas-phase chlorine due to photolysis (Wang et al., 2019, Faxon et al., 2015). In coastal areas and in polluted northern hemisphere areas, the concentration of Cl atoms reaches 1×10^5 atoms cm^{-3} (Pszenny et al., 1993, Spicer et al., 1998, Ezell et al., 2002, Tackett et al., 2007) and 5×10^4 atoms cm^{-3} (Hossaini et al., 2016), respectively, making the reactions of Cl with VOCs a potentially significant elimination route in the atmosphere for these species. Therefore, the study of these processes is necessary to assess the fate of these species in the atmosphere and to better evaluate the atmospheric implications of their oxidation processes.

To our knowledge, the rate coefficient for the T2P+Cl reaction, k_{T2P}, was measured by Rodríguez et al., 2005 by a relative method at room temperature and an atmospheric pressure of air and N_2 in a Teflon bag using the GC-FID (Flame ionization detector).

The value provided by Rodríguez et al., $(1.31\pm0.19)\times10^{-10}$ cm^3 $molecule^{-1}$ s^{-1}, is the only experimental data for k_{T2P}. However, an estimation of k_{T2P}, calculated using the Structure-

Activity Relationships (SARs) method, 3.47×10^{-10} cm^3 $molecule^{-1}$ s^{-1}, is not in agreement with the experimental value (Teruel et al., 2009). This value is close to the gas kinetic limit for such a bimolecular elementary reaction. To elucidate this discrepancy, the present paper describes the determination of the rate coefficient k_{T2P} and aims at evaluating the impact of the Cl + T2P reaction in the removal of T2P in the atmosphere. In addition to the kinetic investigation, the identification and quantification of the gas-phase products and the SOA formation induced by reaction R1 are provided for the first time in the present work.

2. Materials and methods

2.1. Kinetic study

The kinetic study was carried out at 296±2 K and 730±20 Torr of air by a relative method using two set-ups described below.

2.1.1. D-ASC chamber (IMT Lille Douai, France)

A detailed presentation of this experimental set-up can be found elsewhere (Turpin et al., 2006), and only a brief description is given here. The Douai Atmospheric Simulation Chamber (hereafter D-ASC) is a 300-L Teflon bag enclosed inside a wooden box and equipped with a 2-L multiple-reflection optical cell with 10 m of optical path coupled to an FTIR spectrometer (Nicolet 550). The IR spectra of the gaseous samples (T2P and the reference compound and/or reaction products) were recorded with a resolution of 0.5 cm^{-1} in the spectral range 4000-650 cm^{-1} by accumulating 32 interferograms. In our experiments, Cl atoms were generated from the photolysis of molecular chlorine using 1 or 2 actinic lamps (Philips TMX 200 LS, emitting in the range 300-460 nm, λ_{max} = 365 nm), which were fixed on the internal walls of the box. All reactions were studied in purified zero air (relative humidity < 2 ppm, CO and CO_2 < 80 ppb). T2P and the reference compounds were injected

into the Teflon bag using syringes. The sampling was made automatically each 5 min for analysis by FTIR. At the end of each experiment, the Teflon bag and the optical cell were cleaned several times by filling with zero air followed by pumping.

2.1.2. 16-L cell (University of Castilla La Mancha UCLM - Ciudad Real, Spain)

This experimental set-up was described in detail elsewhere (Ballesteros et al., 2009, Sleiman et al., 2014), and only a brief outline is provided here. It consists of a 16-L Pyrex White-type cell that has 96 m of the optical path. The cell is equipped with a Nexus 870 Thermo Nicolet FTIR spectrometer. IR spectra were recorded with a resolution of 2 cm^{-1} in the IR spectral range of 4000 to 650 cm^{-1}. The cell is surrounded by 4 actinic lamps (Philips TL-K 40 W, λ_{max} = 365 nm). All experiments were carried out in synthetic air (purity 99.999%, Air Liquide). The introduction of reactants in the gas-phase was done by expansion from a glass manifold system. At the end of each experiment, the cell was cleaned by filling with air and pumping down to 10^{-2} mbar several times.

2.1.3. Rate coefficient determination

The relative rate coefficient of the gas-phase reaction of T2P with Cl was measured in the presence of a reference compound (isoprene, cyclohexane or ethanol) using either the D-ASC chamber or the 16-L cell. The experimental conditions used in this study are summarized in Table 1. The reactions of interest are the simultaneous reactions of T2P and the reference compound with chlorine atoms, with rate coefficients as k_{T2P} and k_{Ref}, respectively:

$$T2P + Cl \xrightarrow{k_{T2P}} Products \qquad (R1)$$

$$Reference + Cl \xrightarrow{k_{Ref}} Products \qquad (R2)$$

Before starting the kinetic study, tests were carried out to check the stability of T2P and the reference compounds by quantifying dark reactions (loss onto the walls and potential reaction with Cl_2) and photolysis processes. The loss rate coefficients due to dark reactions and to photolysis are defined as $k_{WL,X}$ and $k_{PL,X}$, where X compound could be either T2P or reference compound. The values are summarized in Table 1. The rate coefficients, k_L, accounting for all these secondary loss processes are included in Eq. 1. They typically represent from 6 to 15% of the logarithm components according to the reference compound employed in the experiments. The time evolution of the concentration of T2P and the reference compound is, then, described by the following expression:

$$ln\left(\frac{[T2P]_0}{[T2P]_t}\right) - k_{L,T2P}t = \frac{k_{T2P}}{k_{Ref}}\left[ln\left(\frac{[Ref]_0}{[Ref]_t}\right) - k_{L,Ref}t\right] \qquad (Eq.\ 1)$$

where $[T2P]_0$, $[Ref]_0$ and $[T2P]_t$, $[Ref]_t$ are the concentrations of T2P and the reference compound at times t=0 and t, respectively, and $k_{L,T2P}$ and $k_{L,Ref}$ are the loss rate coefficients due to secondary processes for T2P and the reference compound, respectively. The linear least-square analysis at zero intercept of the $ln([T2P]_0/[T2P]_t) - k_{L,T2P}t$ against $ln([Ref]_0/[Ref]_t) - k_{L,Ref}t$ plot yields k_{T2P}/k_{Ref}. The rate coefficient of T2P toward chlorine atoms k_{T2P} was then calculated using the known rate coefficient k_{Ref}.

During the experiments performed in the D-ASC chamber, isoprene was used as the reference compound considering a Cl-rate coefficient $k_{Isoprene}$ of $(4.80\pm1.25)\times10^{-10}$ cm^3 $molecule^{-1}$ s^{-1}. This value is the average of those provided by (Ragains and Finlayson-Pitts, 1997, Fantechi et al., 1998 and Orlando et al., 2003). In the 16-L cell, two reference compounds were employed: ethanol ($k_{Ethanol}$ = $(1.0\pm0.2)\times10^{-10}$ cm^3 $molecule^{-1}$ s^{-1} (IUPAC, 2006) and cyclohexane ($k_{Cyclohexane}$ = $(2.90\pm1.12)\times10^{-10}$ cm^3 $molecule^{-1}$ s^{-1}). This latter rate coefficient is the average of six values given by (Atkinson and Aschmann, 1985, Wallington et al., 1988, Rowley et al., 1992, Aschmann and Atkinson, 1995, Li and Pirasteh, 2006, Anderson et al.,

2007). The error in k_{Ref} represents twice the standard deviation calculated from the averages of individual k_{Ref}.

The reagents (T2P and the reference compound) consumption in the D-ASC chamber was monitored as a function of time, using the following IR spectral features: 1175-1115 cm^{-1} and 942-855 cm^{-1} for T2P and isoprene, respectively. In the 16-L cell, the IR spectral features used were as follows: 1750-1700 cm^{-1} for T2P, 2890-2830 cm^{-1} for cyclohexane and 930-840 cm^{-1} for ethanol. Once in the reactor, the gas mixture was allowed to stabilize for 40 min in the D-ASC chamber and 10 min in the 16-L cell. Indeed, the stabilization time of reagents is dependent on the volume of the reactor. The initial concentrations of T2P, reference compounds and Cl_2 were obtained based on the injected amounts (D-ASC) or the pressure measurements (16-L cell) and are summarized in Table 1.

The overall error Δk_{T2P} in the individual rate coefficient comes from statistical errors Δk_{T2P} *(stat)* and systematic errors Δk_{T2P} *(syst)* as follows:

$$\Delta k_{T2P} = \sqrt{\Delta k_{T2P}\,(stat)^2 + \Delta k_{T2P}\,(syst)^2} \qquad \textit{(Eq. 2)}$$

Statistical errors Δk_{T2P} *(stat)* are calculated according to the following equation:

$$\frac{\Delta k_{T2P}\,(stat)}{k_{T2P}} = \frac{\Delta(Slope)}{Slope} + \frac{\Delta k_{Ref}}{k_{Ref}} \qquad \textit{(Eq. 3)}$$

$\Delta(Slope)$ comes from the determination of the slope in Eq. 1 and results from the least-squares analysis of Figure 1. Δk_{Ref} is the uncertainty on the rate coefficient of the used reference compounds. In this work, this value represents two standard deviations obtained from the averaging of several values of k_{Ref} found in the literature, as explained above. Systematic errors Δk_{T2P} *(syst)* are estimated to 10%. They come mainly from the uncertainty in measuring the concentrations of the reagents (measurements of the areas of the spectroscopic peaks,

182 possible interference, and temperature instability). To minimize this error, 32 IR spectra were
183 recorded for each experiment.

184 **2.2. Mechanistic study**

185 In independent experiments without adding a reference compound, the products formed
186 during the gas-phase reaction of T2P with chlorine atoms were identified and quantified using
187 two different detection methods: FTIR spectroscopy, coupled to the 16-L cell described
188 above, and GC-MS technique, coupled to the 264-L Pyrex chamber (Ciudad Real-
189 Atmospheric Simulation Chamber, CR-ASC), described below.

190 In the 16-L Pyrex cell, the concentrations of T2P and the formed products were followed in
191 situ by monitoring the evolution of their IR absorption bands. The IR spectral features used
192 for this analysis were as follows: 1180-1120 cm^{-1} for T2P, 875-817 cm^{-1} for propanal, 1840-
193 1780 cm^{-1} for formic acid, 2230-2060 cm^{-1} for CO and 3100-2600 cm^{-1} for HCl. Examples of
194 measured spectra are shown in Figure S1. The identification of the products was done using
195 standard reference libraries of IR spectra.

196 The CR-ASC set-up was presented in detail elsewhere (Ballesteros et al., 2009), and only a
197 brief description is provided here. It consists of a 264-L Pyrex cylindrical reactor with four
198 quartz windows on the sides. The chamber is surrounded by a set of 8 actinic lamps (Philips
199 BL TL 40W/10 1SL/25, emitting in the range 340-400 nm, λ_{max} = 365 nm) used to generate
200 Cl atoms from the photolysis of Cl_2. A GC-MS apparatus (Thermo Electron, Trace GC Ultra
201 and DSQ II) was employed to analyze the gas mixture from the chamber. The Solid-Phase
202 Micro-Extraction (SPME) technique was used for sampling the mixture using a 50/30 μm
203 divinylbenzene/carboxen/polydimethylsiloxane fiber as an absorber. The coated fiber was
204 exposed to the gas mixture during an optimized time of 15 min. The fiber samples were then

thermally desorbed in the heated (at 523 K) GC injection port, and the products were analyzed by GC-MS by using temperature ramps that ranged between 313 and 573 K. The identification of the reaction products was carried out by using the electronic impact ionization mass spectrum of each retention time. The consumption of T2P and the formation of the products were examined by monitoring the areas of corresponding chromatographic peaks observed at a certain retention time. The initial concentration of T2P and Cl_2 used for the mechanistic study are summarized in Table 2. Examples of a chromatogram and obtained mass spectra of the detected products are shown in Figure S2.

2.3. Secondary Organic Aerosol (SOA) study

2.3.1. Experimental apparatus

The set-up used has already been presented elsewhere (Antiñolo et al., 2019). Hence, only a brief description will be given here with a special emphasis on the specificities of the present work. The study of the SOA formation in reaction R1 was carried out at 296±2 K and 730±20 Torr of synthetic air using both the CR-ASC and the 16-L cell described above. Ranges of initial concentrations of T2P and Cl_2 were (1.56-9.23)×10^{14} molecule cm^{-3} and (1.55-15.8)×10^{14} molecule cm^{-3}, respectively. The loss of T2P, necessary to quantify the SOA yield, was measured using the FTIR spectrometer described in section 2.1.2. Cl atoms were generated in the CR-ASC as described in section 2.2.

A Fast Mobility Particle Sizer (FMPS) spectrometer (TSI 3091) was used to measure the number of particles formed with diameters ranging between 5.6 and 560 nm. Although it allows a time resolution of 1 s, averaged values for 1 min were considered in the present investigation. Mass concentrations were determined using an SOA density of 1.4 $g.cm^{-3}$, which corresponds to the recommended value of Hallquist et al., 2009.

The gas mixture from the CR-ASC chamber entered in the FMPS through a 1 μm cut cyclone at a 10 L min^{-1} flow rate, and a 10 L min^{-1} filtered exhaust flow rate from the FMPS was then directed to the 16-L cell for FTIR measurements and then again to the CR-ASC, closing the circuit and allowing mixing of the gases in the system. Data were recorded with both FTIR and FMPS typically during 80 min as follows: 10 min before starting the reaction (dark measurements), 50 min under irradiation, followed by 20 min in dark conditions.

2.3.2. Determination of the SOA production

The SOA yield Y_{SOA} is defined by the following equation:

$$Y_{SOA} = \frac{M_{SOA}}{\Delta[T2P]} \qquad (Eq.\ 4)$$

From the time evolutions of the SOA mass production M_{SOA} and the reactant consumption $\Delta[T2P]$, it is possible to plot M_{SOA} as a function of $\Delta[T2P]$ and determine Y_{SOA} from the slope. Both M_{SOA} and $\Delta[T2P]$ were corrected to account for their loss in the dark when no Cl reaction is taking place, as explained in a previous study (Antiñolo et al. 2019). The loss of M_{SOA} was characterized during the last 20 min of each experiment under the dark conditions from the FMPS measurements, and its rate coefficient was in the $(5.22–6.97)\times10^{-4}$ s^{-1} range. $\Delta[T2P]$ was corrected considering the FTIR measurements of T2P in the first 10 min of the experiment under dark conditions from which it was possible to detect a loss rate coefficient within the $(1.16\text{-}20.8)\times10^{-4}$ s^{-1} range. Tests were also done to confirm that no SOA was formed during the Cl_2 dark reaction or exposure of T2P under the light.

In each experiment, M_{SOA} reaches a maximum value $M_{SOA,max}$, which is directly correlated to the SOA yield Y_{SOA}. Indeed, SOA formation can be described by the one-product model proposed by (Pankow, 1994) for which the following equation was recommended by (Odum et al., 1996):

$$Y_{SOA} = M_{SOA,max}\left(\frac{\alpha K_p}{1 + M_{SOA,max}K_p}\right) \quad (Eq.\ 5)$$

where α is the mass-based gas-phase stoichiometric coefficient of a model product, and K_p represents its gas-particle partitioning equilibrium constant. The present study allows us to obtain these coefficients as explained in the discussion section 3.3.

2.4. Chemicals

The reagents employed were obtained from the following sources: T2P (≥95%, Sigma-Aldrich), isoprene (99%, Sigma-Aldrich), cyclohexane (99.9%, Sigma-Aldrich), ethanol (≥99.5%, Sigma-Aldrich), Cl_2 (10% in N_2, Air Products) at IMT Lille Douai and Cl_2 (99.8%, Sigma-Aldrich) at UCLM.

3. Results and discussion

3.1. Kinetic study

The plots of $ln([T2P]_0/[T2P]_t)$-$k_{L,T2P}t$ vs. $ln([Ref]_0/[Ref]_t)$-$k_{L,Ref}t$ are presented in Figure 1. Relative rate coefficients were obtained for each reference compound. Individual and average k_{2TP} are summarized in Table 3. The good linearity with a correlation coefficient greater than 98% and an intercept close to zero for all the reference compounds indicates that no other secondary reactions occur. The error reported on the average rate coefficient shown in Table 3 is two standard deviations. The overall error Δk_{T2P} in the individual rate coefficient values ranges from 24 to 42%.

Two determinations for the rate coefficient of the studied reaction exist in the literature: an experimental value, $(1.31\pm0.19)\times10^{-10}$ cm^3 $molecule^{-1}$ s^{-1} (Rodríguez et al., 2005), and a rate coefficient estimated using the SAR method, 3.47×10^{-10} cm^3 $molecule^{-1}$ s^{-1} (Teruel et al.,

2009). The present value of $(2.56\pm0.83)\times10^{-10}$ cm^3 $molecule^{-1}$ s^{-1} lays between these two values.

k_{T2P} obtained in the present work is found to be higher than that provided by Rodríguez et al., also obtained using a relative method, by about a factor of 2. In Rodríguez et al.'s work, the losses of T2P and the reference compounds (ethane, propene and 1-butene) were monitored by GC-FID detection. The source of discrepancy with Rodríguez et al.'s work is not clear. First, the Cl-rate coefficients for the reference compounds used by Rodríguez et al. cannot be the reason for this discrepancy. These rate coefficients (in cm^3 $molecule^{-1}$ s^{-1}) were $(5.85\pm0.55)\times10^{-11}$ (Hitsuda et al., 2001), $(2.31\pm0.29)\times10^{-10}$ (Stutz et al., 1998) and $(3.00\pm0.40)\times10^{-10}$ (Orlando et al., 2003) for ethane, propene and 1-butene, respectively. Indeed, a re-evaluation of the value obtained by Rodríguez et al., for k_{T2P} using the rate coefficients recommended by IUPAC, 2006 for ethane and propene (5.9×10^{-11} and 2.70×10^{-10} cm^3 $molecule^{-1}$ s^{-1}, respectively), gives $k_{T2P} = 1.39\times10^{-10}$ cm^3 $molecule^{-1}s^{-1}$, which remains within the error bars given by these authors. The only difference that we can find between the two works, apart of the used technique, is that in Rodríguez et al.'s work the losses were not corrected although that wouldn't explain the discrepancy. It is important to note that in the present work, the rate coefficient of the reaction of T2P with Cl was measured in two different set-ups under different conditions. Very close rate coefficients values were obtained making our reported value reliable. The rate coefficient of the reaction of T2P with Cl atoms estimated by Teruel et al., 2009 using the SAR method is 25% higher than that determined in the present work. The source of this discrepancy is probably the uncertainties of the SAR method that aims to estimate rate coefficients based on the reactivity of other compounds considering only their structure.

As generally observed for VOCs, Cl atoms are more reactive than OH radicals toward these species because they are stronger electrophiles than OH radicals. As expected, then, the rate coefficient for reaction R1 is almost 1 order of magnitude greater than the rate coefficient for the OH + T2P reaction, 3.33×10^{-11} cm^3 $molecule^{-1}$ s^{-1} (average from (Davis et al., 2007) and (Albaladejo et al., 2002)).

In Table 4, the rate coefficients of the reactions of a series of C_3-C_7 unsaturated aldehydes with Cl atoms are displayed. Our result confirms that the structure of unsaturated aldehydes has a very small impact on their reactivity towards Cl atoms, as was previously observed (Ullerstam et al., 2001, Colmenar et al., 2015)) opposite to their reactivity towards OH and NO_3 radicals (Tables S1 and S2). The reactivity towards Cl seems to be fairly independent of the substitution on the olefinic carbons for unsaturated aldehydes, as stated by Blanco et al., 2010.

To evaluate the effect of the –CHO group on the reactivity, a comparison between the reactions of Cl with a series of unsaturated aldehydes to those with the corresponding alkenes would be useful. Unfortunately, no data are available in the literature for the reaction of Cl with *trans*-2-pentene, the corresponding alkene of T2P. However, data for other unsaturated aldehydes and their corresponding alkenes are available. The rate coefficients of the reactions of Cl with crotonaldehyde and 3-methyl-2-butenal (see Table 4) are 34% and 36% lower than those with *trans*-2-butene (3.58×10^{-10} cm^3 $molecule^{-1}$ s^{-1} provided by Kaiser et al., 2007) and 2-methyl-propene (3.38×10^{-10} cm^3 $molecule^{-1}$ s^{-1} provided by Blanco et al., 2010), respectively. This may be due to the negative inductive effect of the carbonyl-containing group, which may deactivate the double bond toward the Cl atom addition. However, this decrease in reactivity due to the electron-withdrawing effect may be compensated by the fact that the –CHO group is a reactive site. This was discussed in the study carried out by

(Thévenet et al., 2000), where the rate coefficient of the reaction of Cl with acrolein (2.2×10^{-10} cm^3 $molecule^{-1}$ s^{-1}) was compared to that for propene (2×10^{-10} cm^3 $molecule^{-1}$ s^{-1}) and was shown to be slightly higher within uncertainties showing that the –CHO group is a reactive site, although H abstraction from the –CHO group remains a minor channel compared to the Cl-addition to the double bond, which is likely to be the major one as stated by these authors.

3.2. Mechanistic study

3.2.1. Molar yields of reaction products

This work represents the first mechanistic study on the T2P+Cl reaction. It has been carried out at 296±2 K and 730±20 Torr of total pressure. By FTIR, HCl, CO, propanal and formic acid were identified and quantified as products formed from the studied reaction (Figure S1). Figure 2 shows a typical concentration vs. time profile for the consumption of T2P and the formation of products. The plots of the $[Product]_t$ vs. $\Delta[T2P]$ for propanal and formic acid are shown in Figure 3. $[Product]_t$ is the product concentration at a time t, $\Delta[T2P]$ is the consumed concentration of T2P at a time t. For propanal, a correction of its concentration was done according to the method described by Ceacero-Vega et al. (2012) and considering the IUPAC recommendation for the rate coefficient of the Cl-reaction of propanal: 1.3×10^{-10} cm^3 $molecule^{-1}$ s^{-1} (Atkinson et al. 2006).

The molar yields obtained from the slopes of the plot depicted in Figure 3 are: (5.2±0.2)% and (6.2±0.4)%, for propanal and formic acid, respectively. The overall errors in the formation yields are due to systematic errors σ_{syst} mentioned above and statistical errors resulting from a least-squares analysis of the $[Product]_t$ vs. $\Delta[T2P]$ plots. CO is expected to be formed as a primary product and also as a final product from the studied reaction and may be generated in the oxidation of other species in the mechanism. For that reason, a molar yield for this

341 compound is not reported in this work. HCl yield is not reported either because it may be a
342 primary product, or it can be generated in the H-abstraction of other reaction products.
343 Propanal is expected to be formed as a primary product from the reaction of T2P with Cl.
344 Formic acid may be produced through the very rapid oxidation of other species generated in
345 the oxidation of T2P or as a consequence of heterogeneous reactions on the chamber walls
346 though no evidence of this phenomenon was observed in our experiments. The residual IR
347 spectrum presented in Figure S1 shows peaks that could correspond to ketene in the 2200-
348 2100 cm^{-1} region, according to Wallington et al. (1996), and 2-chlorobutanal considering the
349 peak typical for a carbonyl group (1750 cm^{-1}), the bands due to C-H bending and stretching
350 (1500-1000 cm^{-1} and 3000-2800 cm^{-1}, respectively) and the band that can correspond to the
351 C-Cl stretching (1000-650 cm^{-1}). However, none of these two compounds could be confirmed
352 by FTIR or quantified given the lack of standards of these products.

353 Three of the peaks observed in the chromatogram obtained by GC-MS could be assigned to
354 reaction products (Figure S2). The peak detected at 4.03 min, for which the mass spectrum
355 (MS) shows peaks at m/z = 106 (molecular ion, M), 78 and 80 (fragment M-CO or M-C_2H_4
356 for the two Cl isotopes), 77 (M-C(O)H), and 41 (C_3H_5), could be assigned to 2-chlorobutanal,
357 and that would confirm the observations made by FTIR. A chlorinated product that could not
358 be identified was observed at 5.09 min retention time: its MS shows the isotopic pattern for Cl
359 in the 77 and 105 peaks, although it was not possible to clearly identify the molecular ion.
360 The last peak in the chromatogram, at 5.82 min, was attributed to 2-pentenoic acid, given that
361 in the MS there are peaks at m/z = 100 (M), 82 (M-H_2O) and 55 (M-C(O)OH). This
362 identification was confirmed by comparing the reference MS library installed in the CG-MS
363 software used in this study. The quantification of these products was not possible due to the
364 lack of standards. However, based on the area of the observed peaks in the chromatogram and
365 assuming the same response for all of them, it seems that the yield of 2-chlorobutanal and the

366 unidentified chlorinated product is higher than that for 2-pentenoic acid (Figure S2). The
367 carbon balance was calculated considering only propanal and CO. The obtained value was
368 shown to not exceed 15% at the end of the reaction showing that additional formed oxidation
369 products could not be detected or quantified.

370 **3.2.2. Proposed reaction mechanism**

371 As other unsaturated aldehydes (Canosa-Mas et al., 2001, Orlando and Tyndall, 2002,
372 Magneron et al., 2002), the degradation of T2P initiated by Cl atoms is expected to proceed
373 via two basic mechanisms: abstraction of the hydrogen atom from the -CHO group and/or
374 addition to the C=C double bond. In Scheme 1, the reaction pathways that may justify the
375 observed products are shown. The addition of a Cl atom may occur on two sites of the C=C
376 double bond: adjacent to the –C(O)H group (α) or on the double-bonded carbon furthest from
377 the aldehydic group (β). As seen in Scheme 1, the α-addition forms the
378 $CH_3CH_2CHCHClC(O)H$ radical, which will react with O_2 followed by a reaction with RO_2 to
379 lead to the corresponding chloroalkoxy radical $CH_3CH_2C(O)HCHClC(O)H$. The
380 decomposition of this chloroalkoxy radical may proceed via two channels. The first one leads
381 to the formation of propanal ($CH_3CH_2C(O)H$), 2-oxoacetylchloride ($ClC(O)C(O)H$), formyl
382 chloride HC(O)Cl and CO. Propanal may further react with Cl atoms to form HCl and
383 $CH_3CH_2C(O)$ radicals (Le Crâne et al., 2004). The second channel leads to the formation of
384 chloromalonaldehyde (C(O)HCHClC(O)H) and acetaldehyde $CH_3C(O)H$. Among these
385 products, only propanal and CO were observed and quantified in this work.
386 The β-addition mechanism proceeds through the $CH_3CH_2CHClCHC(O)H$ radical, which will
387 react with O_2 followed by a reaction with RO_2 to lead to the $CH_3CH_2CHClC(O)HC(O)H$
388 radical. This radical may decompose to lead to the formation of 2-chlorobutanal
389 ($CH_3CH_2CHClC(O)H$) identified by GC-MS, but not quantified and further to the formation
390 of CO identified and quantified by FTIR. The decomposition of the

391 $CH_3CH_2CHClCOHC(O)H$ radical may also lead to the formation of glyoxal (C(O)HC(O)H)
392 and 1-chloropropanal ($CH_3CH_2C(O)Cl$) after the conversion of the reaction of the
393 chloroperoxy radical $CH_3CH_2C(O_2)HCl$ with RO_2. Glyoxal (C(O)HC(O)H) and 1-
394 chloropropanal were not observed in this work, suggesting that this channel either does not
395 occur in the timescale of the experiments or is a minor route in the mechanism. Note also that
396 glyoxal may be readily photolyzed under UV irradiation. The $CH_3CH_2CHClC(O)HC(O)H$
397 radical may react with O_2 to form chloropropylglyoxal ($CH_3CH_2CHClC(O)C(O)H$). This
398 product may be the unidentified one observed by GC-MS but could not be confirmed.
399 The H-abstraction from the –C(O)H group may form the $CH_3CH_2CHCHC(O)$ radical and
400 HCl. In the presence of O_2, the $CH_3CH_2CHCHC(O)$ radical may be converted to the peroxy
401 radical $CH_3CH_2CHCHC(O)O_2$, which generates 2-pentenoic acid ($CH_3CH_2CHCHC(O)OH$)
402 and ozone in the presence of HO_2. 2-pentenoic acid was detected in SPMS/GC-MS analysis.
403 On the other hand, the $CH_3CH_2CHCHC(O)O_2$ radical may also react with RO_2 and generates
404 the $CH_3CH_2CHCHC(O)O$ radical. This radical can decompose to carbon dioxide (CO_2) and
405 ethylvinyl radical (CH_3CH_2CHCH), which is converted to the $CH_3CH_2CHCH(O_2)$ radical in
406 the presence of O_2. The reaction of this later with RO_2 may lead to the formation of butanal
407 ($CH_3CH_2CH_2C(O)H$) not observed in this work. The reaction of $CH_3CH_2CHCH(O_2)$ with
408 RO_2 may also lead to propanal and CO formation, both quantified by FTIR in this work.
409 In the light of the discussion above, the relative contribution of addition and abstraction
410 channels in the suggested mechanism could not be determined. In fact, the product formed
411 only through the β-addition channel and observed in this work (2-chlorobutanal) could not be
412 quantified. Among the products expected to occur from the α-addition channel, only propanal
413 and CO were detected in this work. These products may also be formed through the other
414 channels, as mentioned before.

3.3. SOA study

Figure S3 shows the relationship between the initial concentration of T2P and Cl_2 with $M_{SOA,max}$. A clear dependency of $M_{SOA,max}$ on the amount of Cl_2 introduced in the system was observed, whereas no obvious correlation can be identified with the initial concentration of T2P.

Typical aerosol size distributions at several reaction times for given initial concentrations of T2P and Cl_2 are presented in Figure S4. In Figure 4, the SOA mass concentration M_{SOA} is plotted as a function of the consumed T2P. The SOA yield Y_{SOA} is obtained from linear least-squares analysis. The values of Y_{SOA} are summarized together with the experimental conditions in Table 5. Despite the data scattering (Figure 5), the calculated Y_{SOA} fits reasonably well to a one-product model (Odum et al., 1996), given by Equation 5. A least-square regression on the data gives the following parameters: α = (9.95±2.52)% and K_p = (6.00±2.68) × 10^{-4} m^3 μg^{-1}. Uncertainties are statistics and represent two standard deviations (2σ).

Many products result from the oxidation of a VOC, so this fitting allows for easy comparison of yield curves, but, as reported by Cai and Griffin, 2006, the fitted parameters provide no specific information about the real oxidation products and ascribing meaning to them should be avoided.

The SOA formation yields for the reaction of other unsaturated compounds with Cl have been previously determined. For *trans*-2-methyl-2-butenal, Y_{SOA} were recently determined to be between 0.26 and 1.65% (Antiñolo et al., 2020). These SOA yields are a little lower than the values determined in the present work for the reaction of Cl with T2P.

4. Atmospheric implications and conclusion

The atmospheric lifetime τ_{Cl} of T2P due to its reaction with Cl is estimated from k_{T2P} obtained in this work according to the following equation: $\tau_{Cl} = 1/(k_{T2P} \times [Cl])$. $[Cl]$ represents the global tropospheric concentration of Cl of 1×10^3 atoms cm^{-3} averaged over 24 hours (Wingenter et al., 1999). With this value, a τ_{Cl} of 44 days is calculated. The reaction of T2P with Cl may become significant in coastal areas and in polluted northern hemisphere areas where the concentration of Cl atoms can reach 1×10^5 molecule cm^{-3} (Singh et al., 1996) and 5×10^4 atoms cm^{-3} (Hossaini et al., 2016), respectively, yielding to a lifetime shorter than 1 day which makes the reaction of T2P with Cl a potentially significant elimination route in the atmosphere. The calculated lifetime of T2P due to its reaction with OH is 7 hours using a 24-h average concentration of 1×10^6 molecules cm^{-3} for OH (Atkinson et al., 1997) and the average of the rate coefficient values reported in the literature by (Davis et al., 2007) and (Albaladejo et al., 2002) (3.33×10^{-11} cm^3 $molecule^{-1}$ s^{-1}). A short lifetime (5 hours) of T2P is calculated for its reaction with NO_3 radicals showing that this process is an important removal pathway for T2P during nighttime (Kalalian et al., 2019). These authors provided a lifetime of 9 days towards reaction with ozone. The tropospheric lifetime considering the four chemical removal pathways, is shorter than 3 hours. Further, the UV cross-sections of T2P have been recently determined by Kalalian et al., 2019. A lower limit of 44 min was provided by these authors for the T2P lifetime due to photolysis in the UV solar actinic region. This value was calculated using a quantum yield of unity and a photolysis rate corresponding to June 30 at midday for Paris (zenith angle = 26°). It should be noted however that the overall quantum yield in the actinic region for T2P are not known and that for smaller unsaturated aldehydes such as *trans*-crotonaldehyde it has been found to be quite small since Magneron et al., 2002 obtained an upper value of 0.03 for this species.

461 The degradation products (and molar yields) of T2P in the presence of air were HCl, CO, and
462 propanal (5.2±0.2%). Besides, chlorinated products, such as 2-chlorobutanal, were identified
463 as reaction products of the T2P + Cl reaction but could not be quantified. Highly oxidized
464 compounds, such as 2-pentenoic acid and formic acid (6.2±0.4%), were also detected in this
465 work. Formic acid can be produced as a consequence of heterogeneous reactions on the
466 chamber walls.

467 Given the formation of HCl, the T2P + Cl reaction may contribute to the acidity of marine
468 atmospheres. On the other hand, in polluted areas (high-NO_x conditions), the formation of CO
469 may contribute to photochemical pollution via its OH-reaction, which produces CO_2 and H
470 atoms that quickly combine with O_2 to form HO_2 radicals regenerating OH and producing O_3
471 in the troposphere. It is important to note that in polluted areas, the reaction of T2P with Cl
472 may be a source of other toxic molecules such as PAN type species. In addition, the chemical
473 mechanism displayed in Scheme 1 for NO_x-free conditions will evolve by including RO_2 +
474 NO and RO_2 + NO_2 reactions.

475 As observed in this work, the high particle mass concentration was due to the large amount of
476 T2P present in the system (22.5 ppm). In a real atmosphere, the mixing ratio of T2P is at ppb
477 levels. Considering the small SOA yield formed in the T2P + Cl reaction (Y_{SOA} < 7%), it is
478 not expected that T2P could contribute to the formation of ultrafine particles in clean
479 atmospheres. The dependence of Y_{SOA} with the maximum SOA mass is well-described by a
480 one-product absorptive model that yielded the Odum's parameters α and K_p, the latter being
481 two orders of magnitude lower than the one reported for α-pinene, β-pinene and d-limonene
482 (Cai and Griffin, 2006). Even though the uncertainties in Y_{SOA} are high due to the lack of
483 knowledge in the SOA density, among other assumptions that were made, the determined

SOA yields are in the order of magnitude of those reported for the Cl + toluene reaction (Cai et al., 2008) and other similar biogenic compounds as isoprene (Wang and Ruiz, 2017).

Additionally, insights in the reaction mechanism for the degradation of T2P initiated by Cl atoms were reported here. From the obtained results, the first step of the reaction mechanism seems to proceed mainly by H-abstraction of the aldehydic group and by β-addition of Cl atoms to the double bond. The carbon balance calculated in this study did not exceed 15% at the end of the reaction showing that additional oxidation products could not be detected or quantified. Further studies, with complementary detection techniques, are clearly needed to better understand the mechanism and accurately evaluate the carbon balance and the relative contribution of addition and abstraction channels in this mechanism.

Acknowledgement

The authors are grateful to the INSU-LEFE French program, the IEA program funded by CNRS France and the Brittany Council. IMT Lille Douai acknowledges funding by the French ANR agency under contract No. ANR-11-LabX-0005-01 CaPPA (Chemical and Physical Properties of the Atmosphere), the Région Hauts-de-France, the Ministère de l'Enseignement Supérieur et de la Recherche (CPER Climibio), and the European Fund for Regional Economic Development. This research was also funded by the Consejería de Educación, Cultura y Deportes de la Junta de Comunidades de Castilla-La Mancha through the project SBPLY/19/180501/000052 and the University of Castilla-La Mancha (UCLM) through the project 2019-GRIN-27175 (*Ayudas para la financiación de actividades de investigación dirigidas a grupos).* M. Antiñolo acknowledges UCLM *Plan Propio de Investigación* for funding her research contract.

References

Albaladejo, J., Ballesteros, B., Jiménez, E., Martín, P. and Martínez, E., 2002. A PLP–LIF kinetic study of the atmospheric reactivity of a series of C4–C7 saturated and unsaturated aliphatic aldehydes with OH. Atmospheric Environment, 36(20), pp.3231-3239.

Anderson, R.S., Huang, L., Iannone, R. and Rudolph, J., 2007. Measurements of the 12C/13C kinetic isotope effects in the gas-phase reactions of light alkanes with chlorine atoms. The Journal of Physical Chemistry A, 111(3), pp.495-504.

Angerosa, F., Mostallino, R., Basti, C. and Vito, R., 2000. Virgin olive oil odour notes: their relationships with volatile compounds from the lipoxygenase pathway and secoiridoid compounds. Food Chemistry, 68(3), pp.283-287.

Antiñolo, M., Asensio, M., Albaladejo, J. and Jiménez, E., 2020. Gas-Phase Reaction of trans-2-Methyl-2-butenal with Cl: Kinetics, Gaseous Products, and SOA Formation. Atmosphere, 11(7), p.715.

Antiñolo, M., del Olmo, R., Bravo, I., Albaladejo, J. and Jiménez, E., 2019. Tropospheric fate of allyl cyanide (CH_2CHCH_2CN): Kinetics, reaction products and secondary organic aerosol formation. Atmospheric Environment, 219, p.117041.

Aschmann, S.M. and Atkinson, R., 1995. Rate constants for the gas□phase reactions of alkanes with Cl atoms at 296±2 K. International Journal of Chemical Kinetics, 27(6), pp.613-622.

Atkinson, R. and Aschmann, S.M., 1985. Kinetics of the gas phase reaction of Cl atoms with a series of organics at 296±2 K and atmospheric pressure. International journal of chemical kinetics, 17(1), pp.33-41.

Atkinson, R., Baulch, D.L., Cox, R.A., Hampson Jr, R.F., Kerr, J.A., Rossi, M.J. and Troe, J., 1997. Evaluated kinetic, photochemical and heterogeneous data for atmospheric chemistry: Supplement V. IUPAC Subcommittee on Gas Kinetic Data Evaluation for Atmospheric Chemistry. Journal of Physical and Chemical Reference Data, 26(3), pp.521-1011.

Atkinson, R., Baulch, D. L., Cox, R. A., Crowley, J. N., Hampson, R. F., Hynes, R. G., ... & Subcommittee, I. U. P. A. C. (2006). Evaluated kinetic and photochemical data for atmospheric chemistry: Volume II–gas phase reactions of organic species. *Atmospheric chemistry and physics*, *6*(11), 3625-4055.

Ballesteros, B., Ceacero-Vega, A.A., Garzon, A., Jimenez, E. and Albaladejo, J., 2009. Kinetics and mechanism of the tropospheric reaction of tetrahydropyran with Cl atoms. Journal of Photochemistry and Photobiology A: Chemistry, 208(2-3), pp.186-194.

Bianchi, F., Careri, M., Mangia, A. and Musci, M., 2007. Retention indices in the analysis of food aroma volatile compounds in temperature□programmed gas chromatography: Database creation and evaluation of precision and robustness. Journal of separation science, 30(4), pp.563-572.

Blanco, M.B., Barnes, I. and Teruel, M.A., 2010. FTIR gas-phase kinetic study of the reactions of Cl atoms with $(CH_3)_2C=CHC(O)H$ and $CH_3CH=CHC(O)OCH_3$. Chemical Physics Letters, 488(4-6), pp.135-139.

Cai, X. and Griffin, R.J., 2006. Secondary aerosol formation from the oxidation of biogenic hydrocarbons by chlorine atoms. Journal of Geophysical Research: Atmospheres, 111(D14).

Cai, X., Ziemba, L.D. and Griffin, R.J., 2008. Secondary aerosol formation from the oxidation of toluene by chlorine atoms. Atmospheric Environment, 42(32), pp.7348-7359.

Calvert, J., Mellouki, A., & Orlando, J. (2011). Mechanisms of atmospheric oxidation of the oxygenates.

Canosa-Mas, C.E., Cotter, E.S., Duffy, J., Thompson, K.C. and Wayne, R.P., 2001. The reactions of atomic chlorine with acrolein, methacrolein and methyl vinyl ketone. Physical Chemistry Chemical Physics, 3(15), pp.3075-3084.

Ceacero-Vega, A. A., Ballesteros, B., Bejan, I., Barnes, I., Jiménez, E., & Albaladejo, J. (2012). Kinetics and mechanisms of the tropospheric reactions of menthol, borneol, fenchol, camphor, and fenchone with hydroxyl radicals (OH) and chlorine atoms (Cl). *The Journal of Physical Chemistry A*, *116*(16), 4097-4107.

Cheng, H., Erichsen, H., Soerensen, J., Petersen, M.A. and Skibsted, L.H., 2019. Optimising water activity for storage of high lipid and high protein infant formula milk powder using multivariate analysis. International Dairy Journal, 93, pp.92-98.

Colmenar, I., Martín, P., Cabañas, B., Salgado, S., Tapia, A. and Martínez, E., 2015. Reaction products and mechanisms for the reaction of n-butyl vinyl ether with the oxidants OH and Cl: Atmospheric implications. Atmospheric Environment, 122, pp.282-290.

Davis, M.E., Gilles, M.K., Ravishankara, A.R. and Burkholder, J.B., 2007. Rate coefficients for the reaction of OH with (E)-2-pentenal, (E)-2-hexenal, and (E)-2-heptenal. Physical Chemistry Chemical Physics, 9(18), pp.2240-2248.

Ezell, M.J., Wang, W., Ezell, A.A., Soskin, G. and Finlayson-Pitts, B.J., 2002. Kinetics of reactions of chlorine atoms with a series of alkenes at 1 atm and 298 K: structure and reactivity. Physical Chemistry Chemical Physics, 4(23), pp.5813-5820.

Fantechi, G., Jensen, N.R., Saastad, O., Hjorth, J. and Peeters, J., 1998. Reactions of Cl atoms with selected VOCs: Kinetics, products and mechanisms. Journal of atmospheric chemistry, 31(3), pp.247-267.

Faxon, C. B., Bean, J. K., & Ruiz, L. H. (2015). Inland concentrations of Cl2 and ClNO2 in Southeast Texas suggest chlorine chemistry significantly contributes to atmospheric reactivity. *Atmosphere*, *6*(10), 1487-1506.

Gardner, H.W., Grove, M.J. and Salch, Y.P., 1996. Enzymic pathway to ethyl vinyl ketone and 2-pentenal in soybean preparations. Journal of Agricultural and Food Chemistry, 44(3), pp.882-886.

Graedel, T.E. and Crutzen, P.J., 1986. The role of atmospheric chemistry in environment-development•• Interactions. Sustainable Development of the Biosphere. Clark, WC and Munn, RE (eds.). Cambridge University Press, Cambridge, pp.213-251.

Griffin, R.J., Cocker III, D.R., Flagan, R.C. and Seinfeld, J.H., 1999. Organic aerosol formation from the oxidation of biogenic hydrocarbons. Journal of Geophysical Research: Atmospheres, 104(D3), pp.3555-3567.

Hallquist, M., Wenger, J.C., Baltensperger, U., Rudich, Y., Simpson, D., Claeys, M., Dommen, J., Donahue, N.M., George, C., Goldstein, A.H. and Hamilton, J.F., 2009.

The formation, properties and impact of secondary organic aerosol: current and emerging issues. Atmospheric chemistry and physics, 9(14), pp.5155-5236.

Hatai, M., Horiyama, S., Yoshikawa, N., Kinoshita, E., Kagota, S., Shinozuka, K. and Nakamura, K., 2019. trans-2-Pentenal, an Active Compound in Cigarette Smoke, Identified via Its Ability to Form Adducts with Glutathione. Chemical and Pharmaceutical Bulletin, 67(9), pp.1000-1005.

Hatanaka, A., 1993. The biogeneration of green odour by green leaves. Phytochemistry, 34(5), pp.1201-1218.

Heiden, A.C., Kobel, K., Langebartels, C., Schuh-Thomas, G. and Wildt, J., 2003. Emissions of oxygenated volatile organic compounds from plants Part I: Emissions from lipoxygenase activity. Journal of atmospheric chemistry, 45(2), pp.143-172.

Hitsuda, K., Takahashi, K., Matsumi, Y. and Wallington, T.J., 2001. Kinetics of the reactions of Cl*($^2P_{1/2}$) and Cl($^2P_{3/2}$) atoms with C_3H_8, C_3D_8, n-C_4H_{10}, and i-C_4H_{10} at 298 K. Chemical physics letters, 346(1-2), pp.16-22.

Hoffmann, T., Odum, J.R., Bowman, F., Collins, D., Klockow, D., Flagan, R.C. and Seinfeld, J.H., 1997. Formation of organic aerosols from the oxidation of biogenic hydrocarbons. Journal of Atmospheric Chemistry, 26(2), pp.189-222.

Houk, K. N. (1976). The photochemistry and spectroscopy of β, γ-unsaturated carbonyl compounds. *Chemical Reviews*, *76*(1), 1-74.

Hossaini, R., Chipperfield, M.P., Saiz□Lopez, A., Fernandez, R., Monks, S., Feng, W., Brauer, P. and Von Glasow, R., 2016. A global model of tropospheric chlorine chemistry: Organic versus inorganic sources and impact on methane oxidation. Journal of Geophysical Research: Atmospheres, 121(23), pp.14-271.

IUPAC 2006. URL: http://publications.iupac.org/pac/reports/year/2006/index.html.

Kaiser, E.W., Donahue, C.J., Pala, I.R., Wallington, T.J. and Hurley, M.D., 2007. Kinetics, Products, and Stereochemistry of the Reaction of Chlorine Atoms with cis- and trans-2-Butene in 10− 700 Torr of N_2 or N_2/O_2 Diluent at 297 K. The Journal of Physical Chemistry A, 111(7), pp.1286-1299.

Kalalian, C., Samir, B., Roth, E. and Chakir, A., 2019. UV absorption spectra of trans-2-pentenal, trans-2-hexenal and 2-methyl-2-pentenal. Chemical Physics Letters, 718, pp.22-26.

Kanakidou, M., Seinfeld, J.H., Pandis, S.N., Barnes, I., Dentener, F.J., Facchini, M.C., Dingenen, R.V., Ervens, B., Nenes, A.N.C.J.S.E., Nielsen, C.J. and Swietlicki, E., 2005. Organic aerosol and global climate modelling: a review. Atmospheric Chemistry and Physics, 5(4), pp.1053-1123.

Le Crâne, J.P., Villenave, E., Hurley, M.D., Wallington, T.J., Nishida, S., Takahashi, K. and Matsumi, Y., 2004. Atmospheric chemistry of pivalaldehyde and isobutyraldehyde: Kinetics and mechanisms of reactions with Cl atoms, fate of $(CH_3)_3CC(O)$ and $(CH_3)_2CHC(O)$ radicals, and self-reaction kinetics of $(CH_3)_3CC(O)O_2$ and $(CH_3)_2CHC(O)O_2$ radicals. The Journal of Physical Chemistry A, 108(5), pp.795-805.

Li, Z. and Pirasteh, A., 2006. Kinetic study of the reactions of atomic chlorine with several volatile organic compounds at 240–340 K. International journal of chemical kinetics, 38(6), pp.386-398.

Magneron, I., Thevenet, R., Mellouki, A., Le Bras, G., Moortgat, G.K. and Wirtz, K., 2002. A study of the photolysis and OH-initiated oxidation of acrolein and trans-crotonaldehyde. The Journal of Physical Chemistry A, 106(11), pp.2526-2537.

Martins, R.C., Monforte, A.R. and Silva Ferreira, A., 2013. Port wine oxidation management: A multiparametric kinetic approach. Journal of agricultural and food chemistry, 61(22), pp.5371-5379.

Masella, P., Guerrini, L., Angeloni, G., Spadi, A., Baldi, F. and Parenti, A., 2019. Freezing/storing olives, consequences for extra virgin olive oil quality. International Journal of Refrigeration, 106, pp.24-32.

Moshonas, M.G., MG, M. and PE, S., 1973. Some newly found orange essence components including trans-2-pentenal. Journal of Food Science, 38, pp.360-361.

Odum, J.R., Hoffmann, T., Bowman, F., Collins, D., Flagan, R.C. and Seinfeld, J.H., 1996. Gas/particle partitioning and secondary organic aerosol yields. Environmental Science & Technology, 30(8), pp.2580-2585.

Orlando, J.J. and Tyndall, G.S., 2002. Mechanisms for the reactions of OH with two unsaturated aldehydes: crotonaldehyde and acrolein. The Journal of Physical Chemistry A, 106(51), pp.12252-12259.

Orlando, J.J., Tyndall, G.S., Apel, E.C., Riemer, D.D. and Paulson, S.E., 2003. Rate coefficients and mechanisms of the reaction of cl□atoms with a series of unsaturated hydrocarbons under atmospheric conditions. International Journal of Chemical Kinetics, 35(8), pp.334-353.

Pankow, J.F., 1994. An absorption model of gas/particle partitioning of organic compounds in the atmosphere. Atmospheric Environment, 28(2), pp.185-188.

Pszenny, A.A.P., Keene, W.C., Jacob, D.J., Fan, S., Maben, J.R., Zetwo, M.P., Springer□ Young, M. and Galloway, J.N., 1993. Evidence of inorganic chlorine gases other than hydrogen chloride in marine surface air. Geophysical Research Letters, 20(8), pp.699-702.

Ragains, M.L. and Finlayson-Pitts, B.J., 1997. Kinetics and mechanism of the reaction of Cl atoms with 2-methyl-1, 3-butadiene (isoprene) at 298 K. The Journal of Physical Chemistry A, 101(8), pp.1509-1517.

Rodríguez, D., Rodríguez, A., Notario, A., Aranda, A., Diaz-de-Mera, Y. and Marínez, E., 2005. Kinetic study of the gas-phase reaction of atomic chlorine with a series of aldehydes.

Rodriguez-Kabana, R., Guertal, E.A., Walker, R.H. and Teem, D.H., Auburn University, 2008. 2-Propenal and Related Enal Compounds for Controlling Plant Pests and Weeds in Soil. U.S. Patent Application 12/190,302.

Rowley, D.M., Lesclaux, R., Lightfoot, P.D., Noziere, B., Wallington, T.J. and Hurley, M.D., 1992. Kinetic and mechanistic studies of the reactions of cyclopentylperoxy and cyclohexylperoxy radicals with hydroperoxy radical. The Journal of Physical Chemistry, 96(12), pp.4889-4894.

Rudich, Y., Donahue, N.M. and Mentel, T.F., 2007. Aging of organic aerosol: Bridging the gap between laboratory and field studies. Annu. Rev. Phys. Chem., 58, pp.321-352.

Ruzsanyi, V., Sielemann, S. and Baumbach, J.I., 2002. Determination of VOCs in human breath using IMS. Int. J. Ion Mobility Spectrom, 5, pp.45-48.

Saison, D., De Schutter, D.P., Delvaux, F. and Delvaux, F.R., 2009. Determination of carbonyl compounds in beer by derivatisation and headspace solid-phase microextraction in combination with gas chromatography and mass spectrometry. Journal of Chromatography A, 1216(26), pp.5061-5068.

Seaman, V. Y., Charles, M. J., & Cahill, T. M. (2006). A sensitive method for the quantification of acrolein and other volatile carbonyls in ambient air. *Analytical chemistry*, *78*(7), 2405-2412.

Seco, R., Penuelas, J., & Filella, I. (2007). Short-chain oxygenated VOCs: Emission and uptake by plants and atmospheric sources, sinks, and concentrations. *Atmospheric Environment*, *41*(12), 2477-2499.

Singh, H.B., Thakur, A.N., Chen, Y.E. and Kanakidou, M., 1996. Tetrachloroethylene as an indicator of low Cl atom concentrations in the troposphere. Geophysical Research Letters, 23(12), pp.1529-1532.

Sleiman, C., El Dib, G., Ballesteros, B., Moreno, A., Albaladejo, J., Canosa, A. and Chakir, A., 2014. Kinetics and Mechanism of the Tropospheric Reaction of 3-Hydroxy-3-methyl-2-butanone with Cl Atoms. The Journal of Physical Chemistry A, 118(32), pp.6163-6170.

Spicer, C.W., Chapman, E.G., Finlayson-Pitts, B.J., Plastridge, R.A., Hubbe, J.M., Fast, J.D. and Berkowitz, C.M., 1998. Unexpectedly high concentrations of molecular chlorine in coastal air. Nature, 394(6691), pp.353-356.

Stutz, J., Ezell, M.J., Ezell, A.A. and Finlayson-Pitts, B.J., 1998. Rate constants and kinetic isotope effects in the reactions of atomic chlorine with n-butane and simple alkenes at room temperature. The Journal of Physical Chemistry A, 102(44), pp.8510-8519.

Tackett, P.J., Cavender, A.E., Keil, A.D., Shepson, P.B., Bottenheim, J.W., Morin, S., Deary, J., Steffen, A. and Doerge, C., 2007. A study of the vertical scale of halogen chemistry in the Arctic troposphere during Polar Sunrise at Barrow, Alaska. Journal of Geophysical Research: Atmospheres, 112(D7).

Tandon, K.S., Baldwin, E.A. and Shewfelt, R.L., 2000. Aroma perception of individual volatile compounds in fresh tomatoes (Lycopersicon esculentum, Mill.) as affected by the medium of evaluation. Postharvest biology and technology, 20(3), pp.261-268.

Teruel, M.A., Achad, M. and Blanco, M.B., 2009. Kinetic study of the reactions of Cl atoms with α, β-unsaturated carbonyl compounds at atmospheric pressure and structure activity relations (SARs). Chemical Physics Letters, 479(1-3), pp.25-29.

Thévenet, R., Mellouki, A. and Le Bras, G., 2000. Kinetics of OH and Cl reactions with a series of aldehydes. International Journal of Chemical Kinetics, 32(11), pp.676-685.

Turpin, E., Tomas, A., Fittschen, C., Devolder, P. and Galloo, J.C., 2006. Acetone-h_6 or-d_6 + OH reaction products: Evidence for heterogeneous formation of acetic acid in a simulation chamber. Environmental science & technology, 40(19), pp.5956-5961.

Ullerstam, M., Ljungström, E. and Langer, S., 2001. Reactions of acrolein, crotonaldehyde and pivalaldehyde with Cl atoms: structure–activity relationship and comparison with OH and NO 3 reactions. Physical Chemistry Chemical Physics, 3(6), pp.986-992.

Wallington, T.J., Skewes, L.M., Siegl, W.O., Wu, C.H. and Japar, S.M., 1988. Gas phase reaction of Cl atoms with a series of oxygenated organic species at 295 K. International journal of chemical kinetics, 20(11), pp.867-875.

724 Wallington, T. J., Ball, J. C., Straccia, A. M., Hurley, M. D., Kaiser, E. W., Dill, M., ... &
725 Bilde, M. (1996). Kinetics and mechanism of the reaction of Cl atoms with CH2 CO
726 (Ketene). *International journal of chemical kinetics*, *28*(8), 627-635.

727 Wang, D.S. and Ruiz, L.H., 2017. Secondary organic aerosol from chlorine-initiated
728 oxidation of isoprene. Atmospheric Chemistry and Physics, 17(22).

729 Wang, X., Jacob, D. J., Eastham, S. D., Sulprizio, M. P., Zhu, L., Chen, Q., ... & Liao, H.
730 (2019). The role of chlorine in global tropospheric chemistry. *Atmospheric Chemistry*
731 *and Physics*, *19*(6), 3981-4003.

732 Winer, A. M., Arey, J., Atkinson, R., Aschmann, S. M., Long, W. D., Morrison, C. L., &
733 Olszyk, D. M. (1992). Emission rates of organics from vegetation in California's
734 Central Valley. *Atmospheric Environment. Part A. General Topics*, *26*(14), 2647-
735 2659.

736 Wingenter, O.W., Blake, D.R., Blake, N.J., Sive, B.C., Rowland, F.S., Atlas, E. and Flocke,
737 F., 1999. Tropospheric hydroxyl and atomic chlorine concentrations, and mixing
738 timescales determined from hydrocarbon and halocarbon measurements made over the
739 Southern Ocean. Journal of Geophysical Research: Atmospheres, 104(D17),
740 pp.21819-21828.

741 Yamanishi, T., Kita, Y., Watanabe, K. and Nakatani, Y., 1972. Constituents and composition
742 of steam volatile aroma from Ceylon tea. Agricultural and Biological
743 Chemistry, 36(7), pp.1153-1158.

Tables

Table 1. Experimental conditions used during our kinetic study.

Reactor	Lamps	Compound	Initial concentration ($\times 10^{13}$ molecule cm^{-3})	$k_{WL,X} \pm \sigma_1$ [a] ($\times 10^{-5}$ s^{-1})	$k_{PL,X} \pm \sigma_2$ [a] ($\times 10^{-5}$ s^{-1})
D-ASC	1-2	T2P	5.04 – 15.10	1.73 ± 0.06 – 6.55 ± 0.39	1.85 ± 0.10 – 6.43 ± 0.41
		Isoprene	5.90 – 14.80	0.50 ± 0.12 – 2.42 ± 0.07	0.54 ± 0.16 – 2.68 ± 0.12
		Cl_2	25.00 – 37.26		
16-L cell	4	T2P	46.20 – 93.00	0.48 ± 0.15 – 1.02 ± 0.08	2.95 ± 0.13 – 3.57 ± 0.07
		Cyclohexane	57.60 – 66.00	0.11 ± 0.09 – 1.07 ± 0.21	
		Ethanol	74.40 – 110	1.72 ± 0.07 – 2.08 ± 0.40	
		Cl_2	66.00 – 132		

[a]: uncertainty is ±1σ.

Table 2. Experimental conditions used during the mechanistic study.

Reactor	**Lamps**	**Compound**	**Initial concentration range (× 10^{14} molecule cm^{-3})**
16-L cell (4 runs)	3	T2P	2.78-5.91
		Cl_2	8.34-9.97
CR-ASC (2 runs)	8	T2P	9.05-9.64
		Cl_2	8.34-8.76

Table 3. Rate coefficients for the reaction of T2P with Cl atoms at 296 ± 2 K and 730 ± 20 Torr.

Reactor	**Reference compound**	k_{T2P}/k_{Ref}	$k_{T2P} \pm \Delta k_{T2P}$ [a] (× 10^{-10} cm^3 $molecule^{-1}$ s^{-1})
D-ASC	Isoprene (6 runs)	0.50 ± 0.04	2.40 ± 0.82
16-L Pyrex cell	Cyclohexane (2 runs)	0.79 ± 0.01	2.29 ± 0.92
	Ethanol (3 runs)	2.99 ± 0.08	2.99 ± 0.69
Average			**2.56 ± 0.83** [b]

$k_{Isoprene}$ = (4.8±1.25)×10^{-10} cm^3 $molecule^{-1}$ s^{-1} (see section 2.1.3)
$k_{Ethanol}$ = (1.0±0.2)×10^{-10} cm^3 $molecule^{-1}$ s^{-1} (see section 2.1.3)
$k_{Cyclohexane}$ = (2.90±1.12)×10^{-10} cm^3 $molecule^{-1}$ s^{-1} (see section 2.1.3)
[a] uncertainty calculated according to equations (4-5)
[b] two standard deviations

Table 4. Summary of the rate coefficients for the reactions of a series of C_3-C_7 unsaturated aldehydes with Cl atoms.

Unsaturated aldehyde	k_{Cl} **(× 10^{-10} cm^3 $molecule^{-1}$ s^{-1})**	**Reference**
Acrolein (CH_2=CH-CHO)	2.2 ± 0.3 2.2 ± 0.3 1.8 ± 0.3 2.5 ± 0.7	(Thévenet et al. 2000) (Canosa-Mas et al. 2001) (Ullerstam et al. 2001) (Wang et al. 2002)
Crotonaldehyde (CH_3-CH=CH-CHO)	2.6 ± 0.3 2.2 ± 0.4 3.2 ± 0.9	(Thévenet et al. 2000) (Ullerstam et al. 2001) (Wang et al. 2002)
3-methyl-2-butenal $(CH_3)_2$C=CH-C(O)H	2.48 ± 0.71	(Blanco et al. 2010)
Trans-2-pentenal (CH_3-CH_2-CH=CH-CHO)	1.31 ± 0.19 3.47 **2.53 ± 0.83**	(Rodríguez et al. 2005) (Teruel et al. 2009) (SAR Estimation) **This work**
Trans-2-hexenal (CH_3-CH_2-CH_2-CH=CH-CHO)	1.92 ± 0.22	(Rodríguez et al. 2005)
Trans-2-heptenal (CH_3-CH_2-CH_2-CH_2-CH=CH-CHO)	2.4 ± 0.29	(Rodríguez et al. 2005)

Table 5. Experimental conditions and results obtained for the SOA study.

$[T2P]_0$ ($\times 10^4$ µg m^{-3})	$[Cl_2]_0$ ($\times 10^4$ µg m^{-3})	$\Delta[T2P]$ ($\times 10^4$ µg m^{-3})	$M_{SOA,max}$ ($\times 10^2$ µg m^{-3})	Y_{SOA} [a] (%)
8.03	1.86	1.80	1.20	0.82 ± 0.02
9.39	2.43	1.75	1.75	1.15 ± 0.02
13.14	4.28	3.08	3.42	1.34 ± 0.02
3.30	3.16	1.56	3.39	2.07 ± 0.09
12.62	8.45	4.75	9.11	2.15 ± 0.02
2.23	2.43	0.88	2.56	2.47 ± 0.08
5.75	8.07	3.36	8.18	2.59 ± 0.05
3.05	8.07	1.67	8.20	2.79 ± 0.08
2.99	8.33	1.62	9.72	3.79 ± 0.10
5.75	7.89	2.19	8.97	3.79 ± 0.10
9.32	13.74	2.79	13.48	4.26 ± 0.11
6.69	12.41	4.31	15.89	4.62 ± 0.27
2.23	7.00	1.35	9.88	4.77 ± 0.28
7.89	18.97	4.89	21.56	5.17 ± 0.39
6.59	16.10	4.43	16.62	5.24 ± 0.54
9.32	17.34	2.46	19.00	6.16 ± 0.10

[a] Y_{SOA} is determined from the slope of $M_{SOA,max}$ vs. Y_{SOA}. Errors are 2σ.

Figure and Scheme Legends

Figure 1. Plot of $ln([T2P]_0/[T2P]_t)-k_{L,T2P}t$ vs. $ln([Ref]_0/[Ref]_t)-k_{L,Ref}t$ according to Eq. 1. Data obtained using the D-ASC (isoprene) and the 16L-cell (Cyclohexane and Ethanol).

Figure 2. Concentration-time profiles for T2P and the major products observed by FTIR using the 16-L cell.. Initial concentrations: 5.91×10^{14} molecule.cm^{-3} for T2P and 9.09×10^{14} molecule.cm^{-3} for Cl_2.

Figure 3. Product yields for HC(O)OH and propanal.

Figure 4. SOA mass concentration M_{SOA} produced from the T2P+Cl reaction as a function of the consumed T2P with an initial concentration of 4.03×10^{14} molecule.cm^{-3} for T2P and 6.72×10^{14} molecule.cm^{-3} for Cl_2. The SOA yield Y_{SOA} is obtained from a linear least-squares analysis.

Figure 5. Plot of SOA yield Y_{SOA} as a function of $M_{SOA,max}$ for the reaction between T2P and Cl.

Scheme 1. Proposed mechanism for the reaction of T2P with Cl atom: α-addition (a), β-addition (b) and H-abstraction (c).

Figures

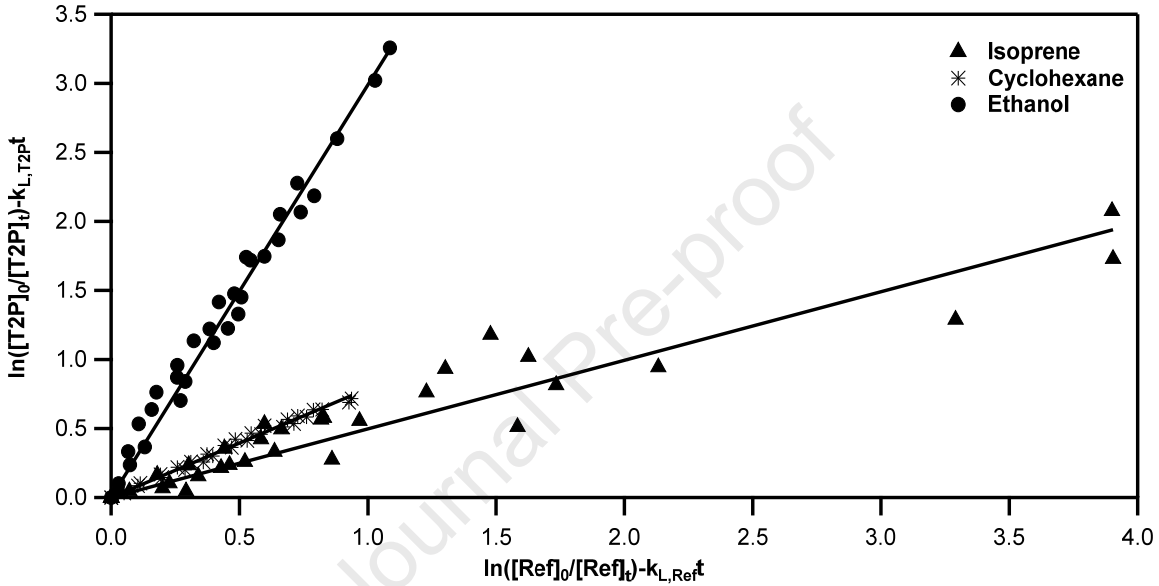

Figure 1. Plot of $ln([T2P]_0/[T2P]_t)-k_{L,T2P}t$ vs. $ln([Ref]_0/[Ref]_t)-k_{L,Ref}t$ according to Eq. 1.

Data obtained using the D-ASC (isoprene) and the 16L-cell (Cyclohexane and Ethanol).

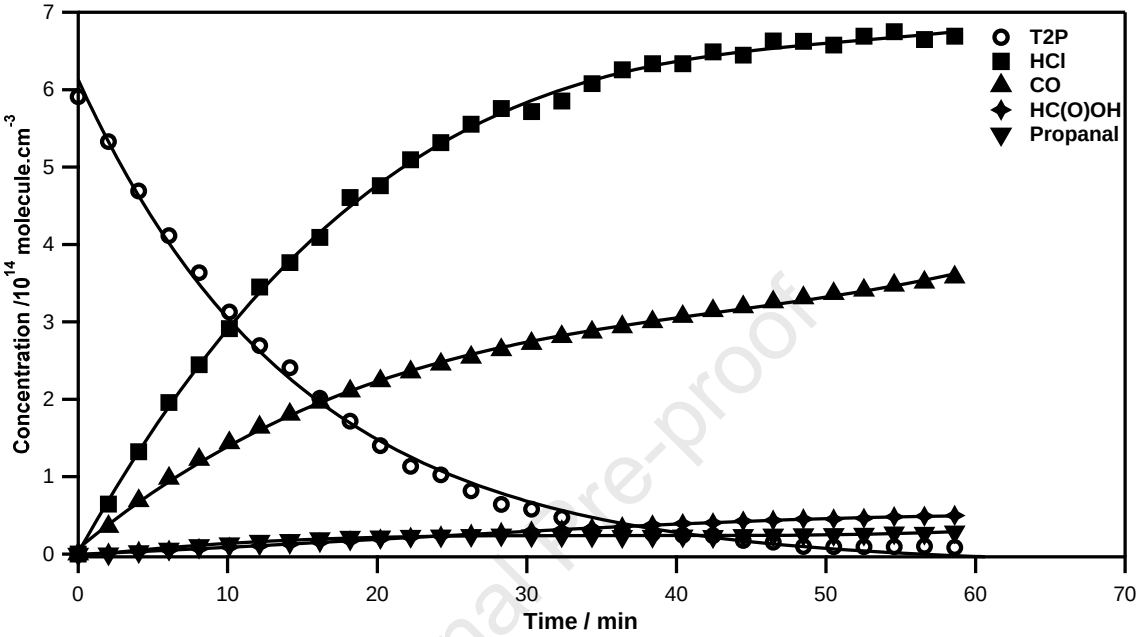

Figure 2. Concentration-time profiles for T2P and the major products observed by FTIR using the 16-L cell. Initial concentrations: 5.91×10^{14} molecule.cm^{-3} for T2P and 9.09×10^{14} molecule.cm^{-3} for Cl_2.

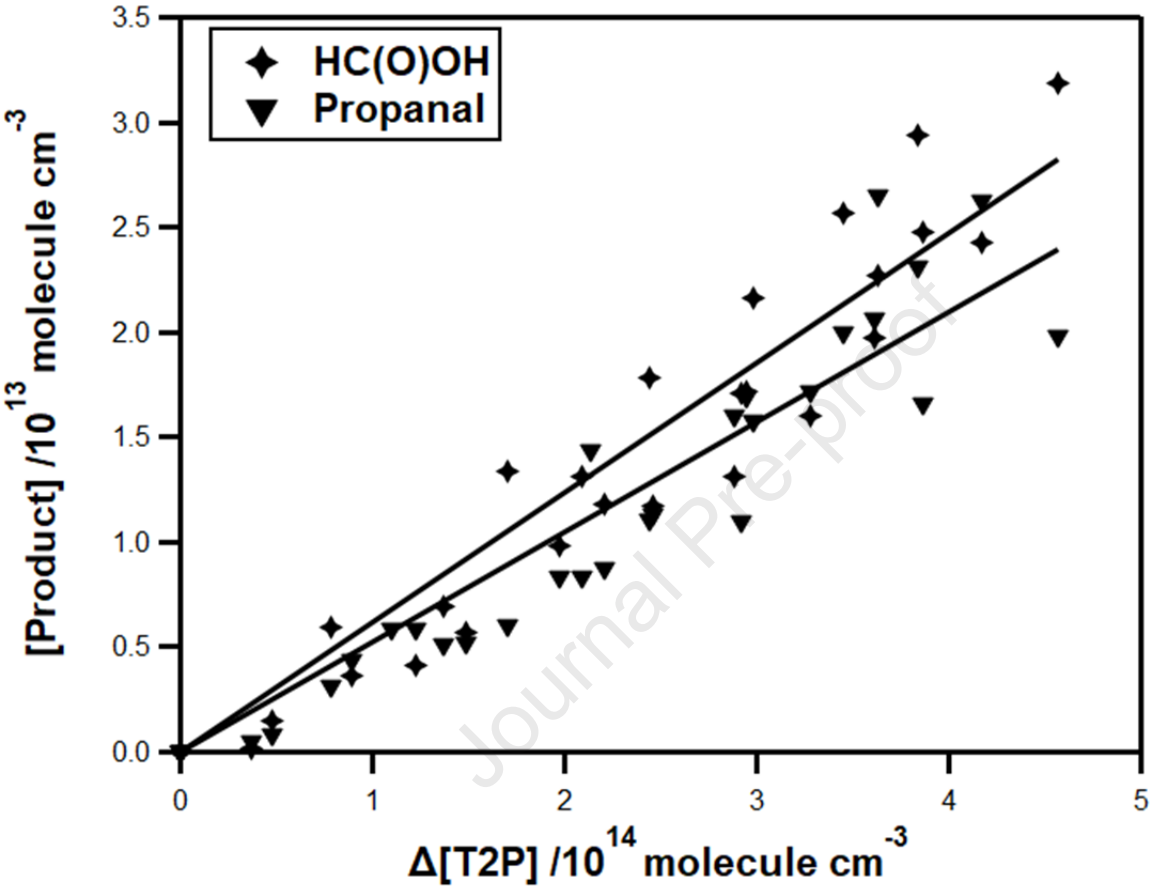

Figure 3. Product yields for HC(O)OH and propanal.

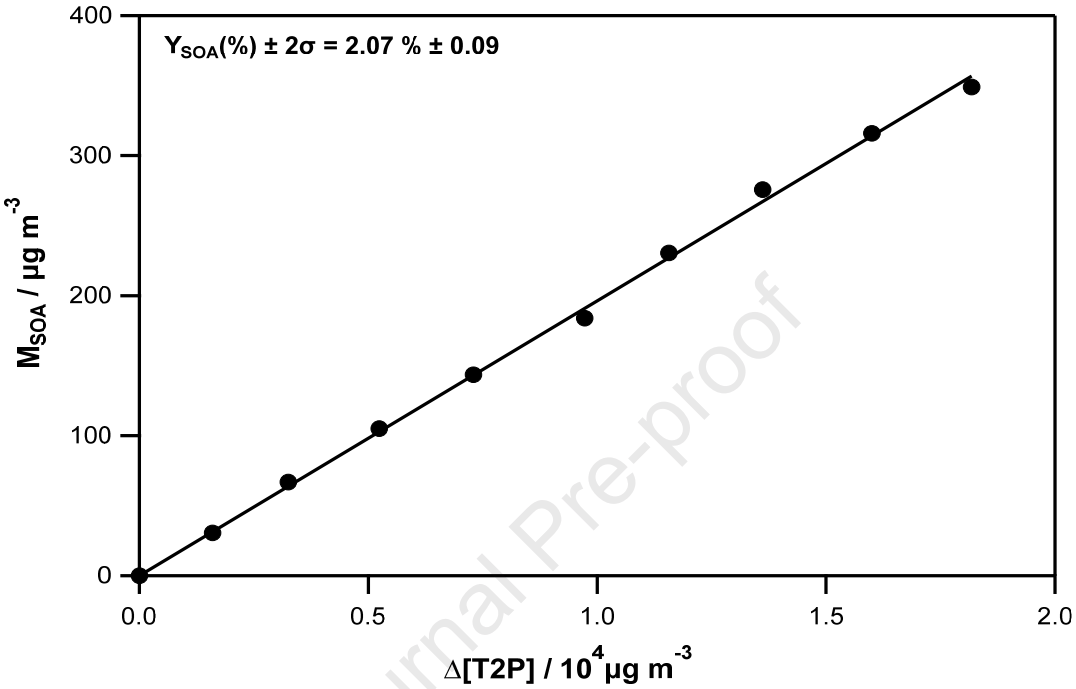

Figure 4. SOA mass concentration M_{SOA} produced from the T2P+Cl reaction as a function of the consumed T2P with an initial concentration of 4.03×10^{14} molecule.cm^{-3} for T2P and 6.72×10^{14} molecule.cm^{-3} for Cl_2. The SOA yield Y_{SOA} is obtained from a linear least-squares analysis.

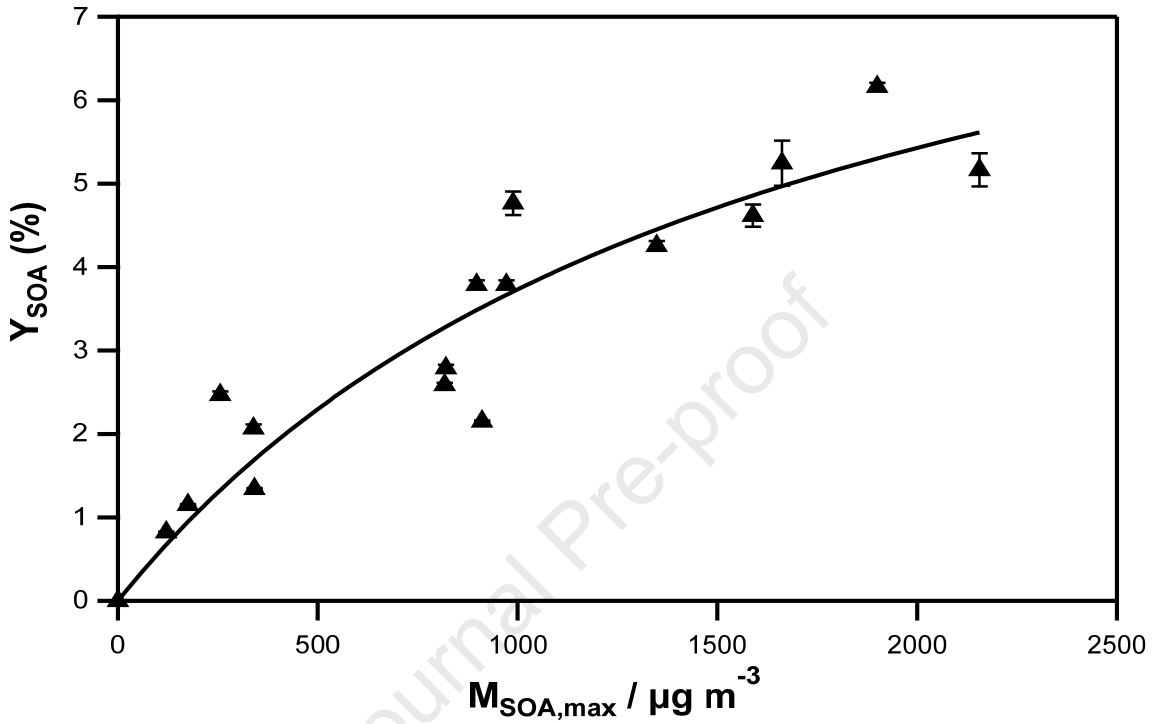

Figure 5. Plot of SOA yield Y_{SOA} as a function of $M_{SOA,max}$ for the reaction between T2P and Cl.

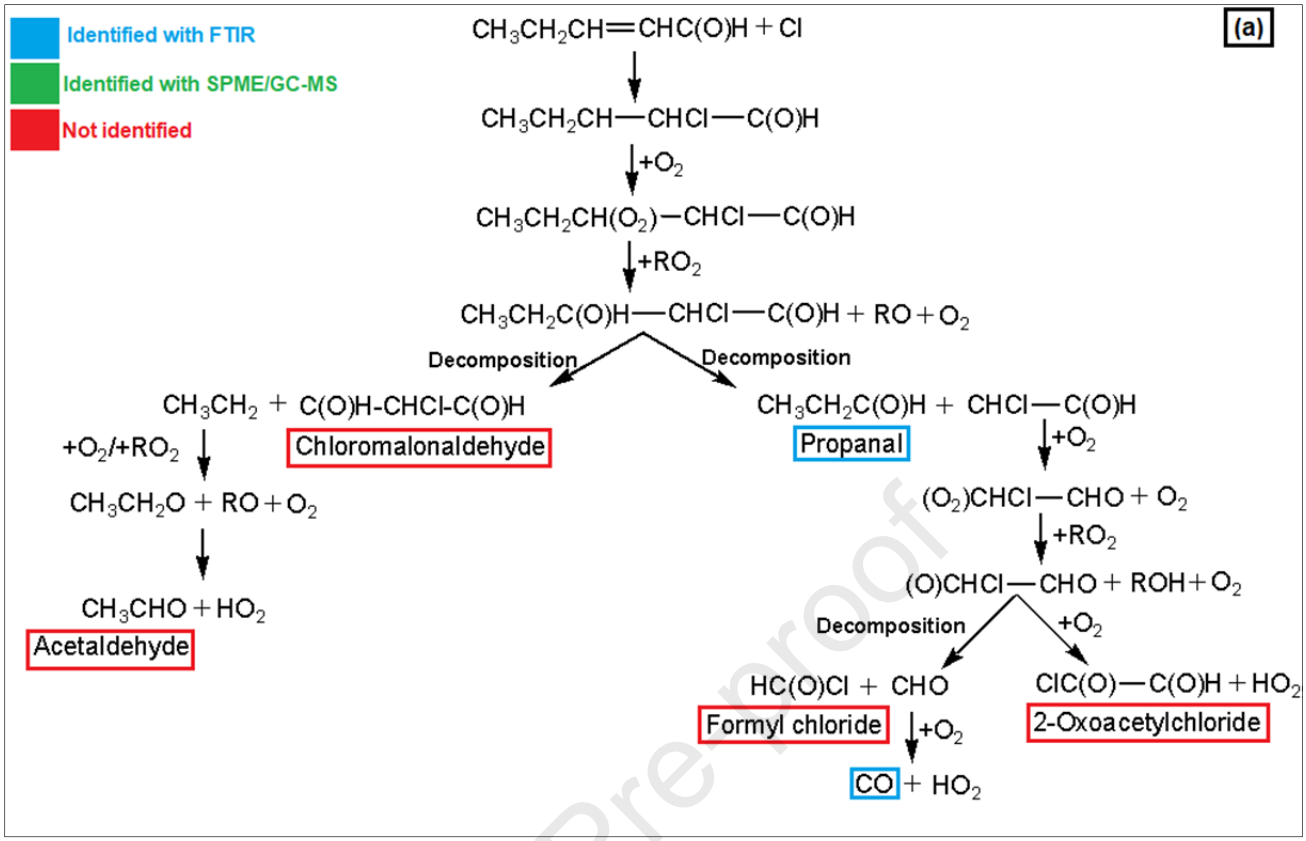

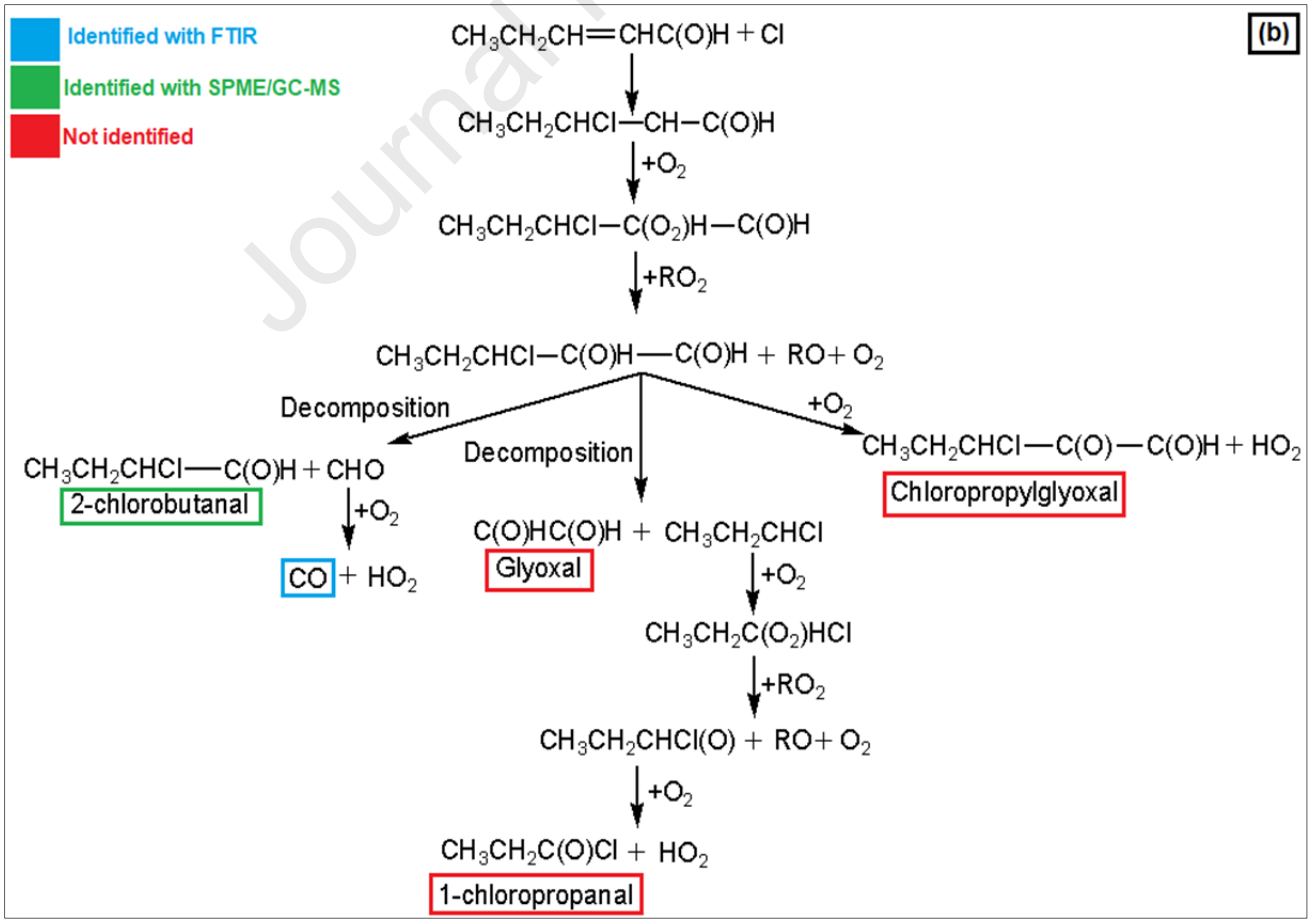

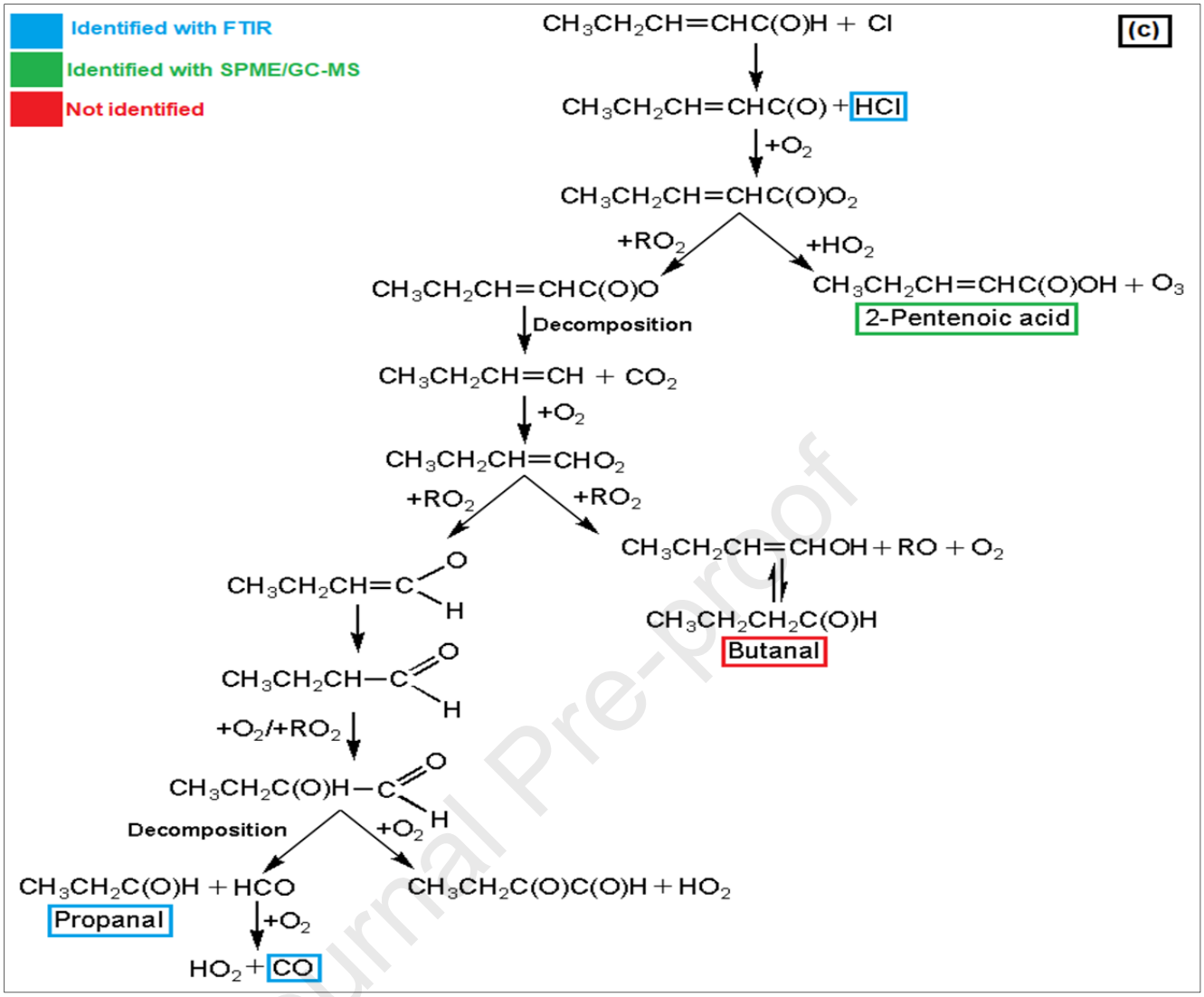

Scheme 1. Proposed mechanism for the reaction of T2P with Cl atom: α-addition (a), β-addition (b) and H-abstraction (c).

- A rate coefficient of (2.56±0.83)×10^{-10} cm^3 $molecule^{-1}$ s^{-1} was obtained for the reaction of T2P with Cl atoms under atmospheric conditions.
- This work is the first study of the gas-phase products and the SOA formation from the reaction of T2P with Cl.
- The T2P + Cl reaction may contribute to the acidity of marine atmospheres.
- The T2P + Cl reaction proceeds mainly by H-abstraction of the aldehydic group and by β-addition of Cl atoms to the double bond.
- Atmospheric lifetimes of T2P toward chemical removals are of few hours.

Declaration of interests

☒ The authors declare that they have no known competing financial interests or personal relationships that could have appeared to influence the work reported in this paper.

☐The authors declare the following financial interests/personal relationships which may be considered as potential competing interests: